Searching for Non-Axisymmetry in 49 Ceti's Unusual Gas-Rich Debris Disk

Cail Daley, Wesleyan University

Advisor: Meredith Hughes, Wesleyan University

Abstract

49 Ceti, a 40 million year old A1V type star 61 parsecs from Earth, is one of only a handful of systems known to retain its molecular gas well into the debris disk phase—the origin of the abnormally high levels of gas in its disk remains a mystery. The degree of axisymmetry of the gas disk can provide clues as to the origin of the gas, which in turn allows new insight into how gas-rich debris disks retain such large amounts of gas for so long. If the gas is axisymmetric, it implies a steady-state evolution (consistent with primordial origin or ongoing evaporation of cometary bodies), but if it is non-axisymmetric, it provides evidence for a recent collision of Mars-sized planetary bodies or resonances induced by a giant planet. Because 49 Ceti is viewed at a high inclination relative to Earth, it is necessary to account for the viewing geometry by performing a "deprojection" of the interferometric data (or visibilities) that assumes an underlying circular geometry before the axisymmetry can be assessed. We extend the functionality of Professor Meredith Hughes' old visibility deprojection code, rewriting it in Python and updating it so that it can include spectral lines— previously it could only handle continuum. We use this code to analyze Atacama Large Millimeter Array (ALMA) observations of the distribution of gas and dust in 49 Ceti's disk, and find the gas to be predominantly axisymmetric, lending credence to a steady-state evolution theory.

Introduction

Young stars are almost always accompanied by circumstellar disks, objects primarily made up of gas that are responsible for the formation of planets (Dutrey et al. 2014, and references within). Over time, accretion, planet formation, and photoevaporation deplete protoplanetary disks as they become gas-poor debris disks; studies have shown that 50% of protoplanetary disks disappear by 3 Myr, and a negligible amount remain by 10 Myr (Wyatt et al. 2015, Hollenbach et al. 1994; Haisch et al. 2001, Hernández et al. 2007). Debris disks are seperated from protoplanetary disks by the second-generation origin of their dust, which tends to be optically thick in protoplanetary disks but optically thin in debris disks. Debris disks tend to lack significant amounts of gas and can last for billions of years (Thureau et al. 2014; Matthews et al. 2014).

49 Ceti, a main-sequence A1V star, hosts a well-studied example of a debris disk, and was recently identified as a likely member of the 40 Myr Argus Association (Zuckerman & Song 2012). 49 Ceti also stands out as being one of only three debris disks to show substantial amounts of submillimeter CO emission; the other two are HD 21997 and β Pictoris (Zuckerman et al. 1995; Hughes et al. 2008; Moór et al. 2011; Dent et al. 2014). As gas is thought to disappear before disks reach the debris disk phase, 49 Ceti presents somewhat of a conundrum. There are two main theories as to the origin of gas in debris disks: Hughes et al. (2008) posit that 49 Ceti's gas could be primordial, and that its disk is in the late stages of transition between gas-rich protoplanetary disk and gas-poor debris disk. However, the age estimate has since been revised from 12 to 40 Myr, making the primoridal scenario unlikely if the identification of 49 Ceti with the co-moving

Argus Association is correct. It is also possible that 49 Ceti's gas is of a second-generation origin and is replenished evenly throughout the disk by planetesimals. Second-generation gas could also be produced by a recent collision between planetary bodies, depositing large amounts of gas on one side of the disk (Zuckerman & Song 2012; Dent et al. 2014). Because different processes deposit gas across the disk in different ways, it is possible to learn about the origin of 49 Ceti's gas by assessing its axisymmetry. In this paper, we will assess 49 Ceti's axisymmetry in an attempt to learn more about the origin of the unusually high concentrations of gas in its disk.

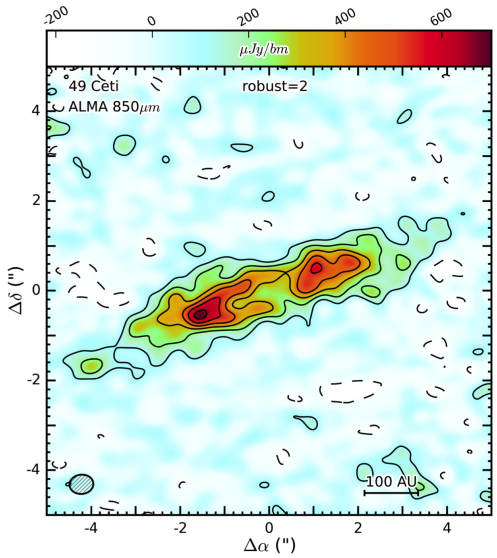

Fig. 1.—: 49 Ceti as seen at 850 μm. Countours are [-2,2,4,6...] $\times$ 55 μJy/beam, the rms noise. The image has a beam size (spatial resolution) of 0.54$''$ $\times$ 0.43$''$, as illustrated by the ellipse in the bottom left corner.

Methods & Analysis

The data used in this paper were taken in November 2013 with ALMA. 45 minutes were spent observing continuum emission from the dust disk and CO(3-2) emission at a spectral resolution of 53 m/s from the gas disk. The data were taken with 28 antennas. Analysis of 49 Ceti's axisymmetry is made difficult by its high viewing inclination from Earth, which has a best fit value of 79.3° (Lieman-Sifry 2015). To make it easier to assess such axisymmetry, we use a deprojection code to create images of the disk as though seen with a inclination of 0. This is done by assuming a circular geometry and "shrinking" the disk's visibilities along the semi-major axis in u-v plane, which "stretches" the disk along the semi-minor axis in the sky plane. It is necessary to know the disk's position angle (PA) and inclination (i) to perform this operation. If (u, v) is a point in the u-v plane, the process of deprojection is described by:

$$\begin{aligned}(u_1, v_1) &= ([u_0 cos(PA) - v_0 sin(PA)]cos(i), u_0 sin(PA) + v_0 cos(PA)) \\ (u_2, v_2) &= (u_1 cos(-PA) - v_1 sin(-PA), u_1 sin(-PA) + v_1 cos(-PA))\end{aligned} \quad (1)$$

(Lay et al. 1997; Kalman 2008) where the first line rotates to a PA of 0 and deprojects, and the last line rotates back to the original position angle. Deprojection also allows radial averaging, as points

equidistant from the center of the disk are also equidistant in the deprojected u-v plane. We plot flux density as a function of deprojected distance, binning the visibilities to mitigate the effects of noise (Figure 2). To calculate the error bars for the flux density in each bin, it is necessary to apply an equation for the weighted standard error of the mean, of the form:

$$(SEM_w)^2 = \frac{N}{(N-1)sumW_i)^2}[\sum(W_i Re_i - \bar{W}\bar{Re}_w)^2$$

$$- 2\bar{Re}_w \sum(W_i - \bar{W})(W_i Re_i - \bar{W}\bar{Re}_w) \quad (2)$$

$$+ \bar{Re}_w^2 \sum(W_i - \bar{W})^2]$$

(Gatz & Smith 1995) where N is the number of visibilities, W_i the weight for sample i, Re_i the visibility for sample i, $\bar{Re}_w$ the weighted mean of the visibilities over samples $i = 1 - N$, $\sum(W_i Re_i)/\sum W_i$, and $\bar{W}$ the mean of the the weights.

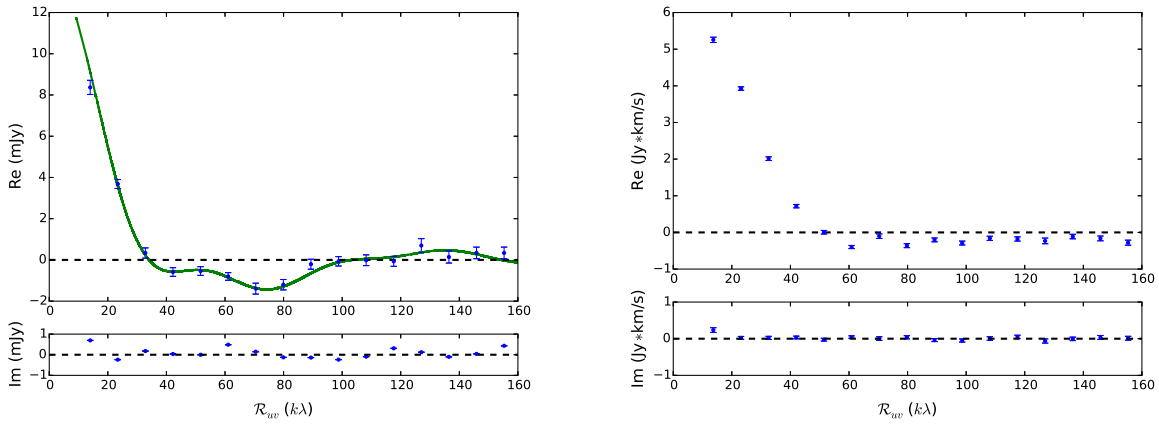

Fig. 2.—: Real and imaginary continuum (right) and line emission (left) flux density as a function of radially averaged deprojected distance from the center of the disk. 1σ uncertainties are represented by the blue error bars. The continuum data are overplotted with a best fit model of the 49 Ceti disk (green line).

Results & Conclusion

We use the deprojection code to image the deprojected disk, allowing us to assess axisymmetry. However, stretching the visibilities also stretches the spatial resolution (known as the beam). This creates an elongated beam, causing the flux of the disk to be smeared along the beam's semi-major axis when it is convolved with the true sky brightness distribution (Figure 3: top). This smearing makes it nearly impossible to assess axisymmetry, so we apply a Gaussian taper to the visibilities (Figure 3: bottom). The Gaussian taper is elongated along the semi-minor axis of the beam, so that when combined with the beam a more circular beam is synthesized at the expense of spatial resolution.

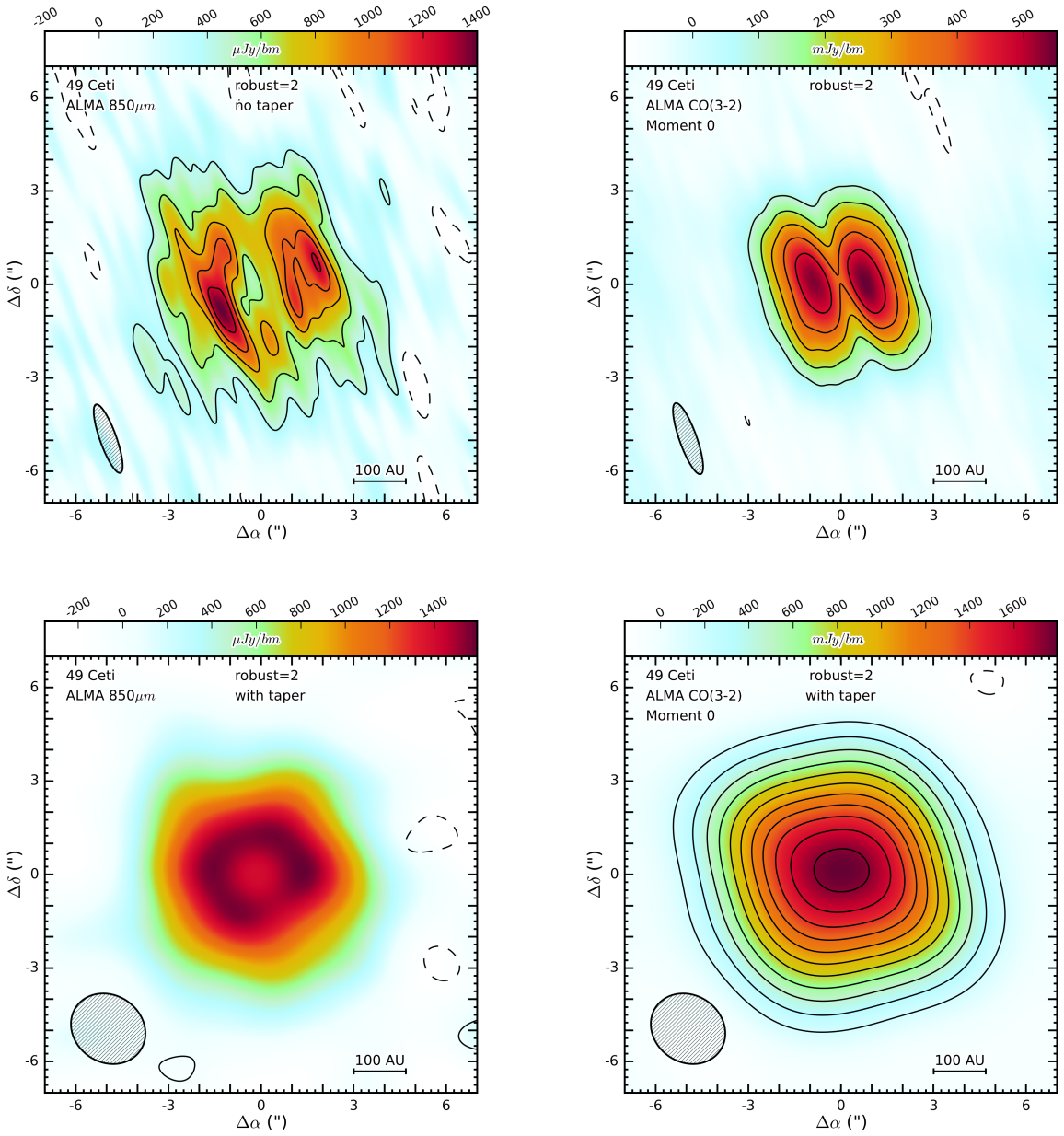

Fig. 3.—: (top left) 49 Ceti deprojected continuum data. Countours are [-2,2,4,6...] × 56 μJy/beam. The beam is 2.32″ × 0.53″. (top right) Deprojected line emission data. Countours are [-2,2,4,6...] × 47 mJy/beam. The beam is 2.42″ × 0.56″. (bottom left) Deprojected continuum data after applying a Gaussian taper. Countours are the residuals of the best fit model subtracted from the data in the visibility domain, and are [-2,2] × 94 μJy/beam. The beam is 2.44″ × 2.11″. (bottom right) Deprojected line emission data after applying a Gaussian taper. Countours are [-2,2,4,6...] × 79 mJy/beam. The beam is 2.50″ × 2.16″. There are no significant departures from axisymmetry in the deprojected & tapered images.

We find that 49 Ceti's gas disk does not show any significant deviations from axisymmetry. This implies that the gas has a steady-state origin, either primordial or one in which planetesimals are a second-generation source of gas. Such gas could be produced by processes such as outgassing of comet-like bodies, photodesorption of ice-coated grains, and grain-grain collisions (Roberge et al. 2013; Lagrange et al. 1998; Chen et al. 2007; Czechowski & Mann 2007). The axisymmetric best-fit model of Lieman-Sifry (2015) fits both the radially averaged deprojected flux density plot and the deprojected and tapered CO(3-2) map well, providing further evidence that 49 Ceti's disk is axisymmetric. Axisymmetry in gas-rich debris disks seems to be common; three newly surveyed A star disks with gas have all been found to be axisymmetric (Capenter et al. in prep). HD 21997 also does not appear to significantly deviate from axisymmetry; only β Pictoris seems to exhibit significant axisymmetric features, with a large clump visible in both CO(3-2) and dust emission seen in the southwest part of the disk (Moór et al. 2011; Dent et al. 2014). This trend of axisymmetry in gas-rich debris disks implies that gas in such disks is often either of primordial origin, or is replenished by steady-state processes rather than collisions of large planetesimals.

I would like to thank my endlessly patient and helpful research advisor Meredith Hughes, who also wrote the original deprojection code that my code was based on. I would also like to thank Jesse Lieman-Sifry for helping me through countless conceptual and coding-related problems. We gratefully acknowledge support from NSF grant AST-1412647, Wesleyan University's Summer Research in Sciences Fellowship, and the Connecticut Space Grant. This paper makes use of the following ALMA data: ADS/JAO.ALMA2012.1.00195.5.

References

Andrews, S. M. 2015
Carpenter, J. M., Gorti, U., Hughes, A. M. 2015, in prep
Chen, C. H., Li, A., Bohac, C., et al. 2007, ApJ, 667, 466
Czechowski, A., & Mann, I. 2007, ApJ, 660, 1541
Dutrey, A., Semenov, D., Chapillon, E., et al. 2014, Protostars and Planets VI, 317
Dent, W. R. F., Wyatt, M. C., Roberge, A., et al. 2014, Science, 343, 1490
Gatz, D. F., Smith, L. 1995, Atmospheric Environment 29, 1185
Haisch, K. E., Jr., Lada, E. A., & Lada, C. J. 2001, ApJ, 553, L153
Hernández, J., Calvet, N., Briceño, C., et al. 2007, ApJ, 671, 1784
Hollenbach, D., Johnstone, D., Lizano, S., & Shu, F. 1994, ApJ, 428, 654
Hughes, A. M., Wilner, D. J., Kamp, I., & Hogerheijde, M. R. 2008, ApJ, 681, 626
Kalman, D. 2008, JOMA Volume 8 Article ID 1663
Lay, O. P., Carlstrom, J. E., & Hills, R. E. 1997, ApJ, 489, 917
Lagrange, A. M., Beust, H., Mouillet, D., et al. 1998, A&A, 330, 1091
Lieman-Sifry, J. 2015, Wesleyan University Honors Thesis
Matthews, B. C., Krivov, A. V., Wyatt, M. C., Bryden, G., & Eiroa, C. 2014, Protostars and Planets VI, 521
Moór, A., Ábrahám, P., Juhász, A., et al. 2011, ApJ, 740, L7
Roberge, A., Kamp, I., Montesinos, B., et al. 2013, ApJ, 771, 69
Thureau, N. D., Greaves, J. S., Matthews, B. C., et al. 2014, MNRAS, 445, 2558
Wyatt, M. C., Panić, O., Kennedy, G. M., & Matrà, L. 2015, Ap&SS, 357, 103
Zuckerman, B., Forveille, T., & Kastner, J. H. 1995, Nature, 373, 494
Zuckerman, B., & Song, I. 2012, ApJ, 758, 77